IEEE Access
Multidisciplinary : Rapid Review : Open Access Journal

Received August 31, 2020, accepted September 4, 2020, date of publication September 7, 2020, date of current version September 25, 2020.

Digital Object Identifier 10.1109/ACCESS.2020.3022523

Adaptive Model-Free Control With Nonsingular Terminal Sliding-Mode for Application to Robot Manipulators

JINSUK CHOI[1], (Student Member, IEEE), JAEMIN BAEK[2], (Member, IEEE), WOONGYONG LEE[3], YOUNG SAM LEE[4], (Senior Member, IEEE), AND SOOHEE HAN[1], (Senior Member, IEEE)

[1]Department of Creative IT Engineering, Pohang University of Science and Technology, Pohang 37673, South Korea
[2]Department of Mechanical Engineering, Gangneung-Wonju National University (GWNU), Wonju 26403, South Korea
[3]Nueromeka, Seoul 04782, South Korea
[4]Department of Electrical Engineering, Inha University, Incheon 22212, South Korea

Corresponding author: Soohee Han (soohee.han@postech.ac.kr)

This work was supported in part by ITECH R&D Program of MOTIE/KEIT Project (No. 20009396), in part by the Industrial Fundamental Technology Development Program of the Ministry of Trade, Industry and Energy, South Korea under Grant 10062312, and in part by Institute for Information and Communications Technology Promotion under Grant 2019-0-00762 (Next-Generation Multistatic Radar Imaging System for Smart Monitoring) funded by the Ministry of Science and Information & Communication Technology (ICT), South Korea.

ABSTRACT An adaptive model-free control with nonsingular terminal sliding-mode (AMC-NTSM) is proposed for high precision motion control of robot manipulators. The proposed AMC-NTSM employs one-sample delayed measurements to cancel nonlinearities and uncertainties of manipulators and to subsequently obtain sufficiently simple models for easy control design. In order to maintain high gain controls even when the joint angles are close to the reference target values and accordingly achieve high precision and fast response control, a nonlinear sliding variable is also adopted instead of a linear one, asymptotically stabilizing controls by guaranteeing even a finite-time convergence. In addition, sliding variables are reflected on control inputs to support fast convergence while achieving uniform ultimate boundedness of tracking errors. The control gains of the proposed AMC-NTSM are adaptively adjusted over time according to the magnitude of the sliding variable. Such adaptive control gains become high for fast convergence or low for settling down to steady motion with better convergence precision, when necessary. The switching gains of the proposed AMC-NTSM are also adaptive to acceleration such that inherent time delay estimation (TDE) errors can be suppressed effectively regardless of their magnitudes. The simulation and experiment show that the proposed AMC-NTSM has good tracking performance.

INDEX TERMS Adaptive control, time-delay control, time-delay estimation, nonsingular terminal sliding-mode, robot manipulator.

I. INTRODUCTION

For a long time, robot manipulators have been successfully developed to achieve high-precision control performance. Nevertheless, more accurate and effective control of robot manipulators is desirable because their higher precision control is still required in various precision engineering fields including even nano- and bio-technology. Recently, extensive research on control of robot manipulators has been conducted to facilitate practical implementation as well as good control performance [1]–[6].

As a practical and effective model-free control of robot manipulators, time-delay control (TDC) schemes combined with auxiliary sliding mode controls (SMCs), such as conventional SMCs [13], second-order SMCs [14], boundary-layer SMCs [15], and adaptive SMCs [16], have been proposed to enhance the tracking performance with a simple control structure, which is herein termed model-free controls with sliding-mode (MC-SMs). Since some research has recently studied advanced SMCs such as robust SMCs [7], terminal SMCs [8]–[10], and disturbance observer(DOB) based SMCs [11], [12], such practical MC-SMs are expected to continue to evolve. By using one-sample delayed measurements to cancel nonlinearities and uncertainties of robot manipulators,

The associate editor coordinating the review of this manuscript and approving it for publication was Hai Wang.

the MC-SMs are designed without mathematical models. Involved auxiliary SMCs of the MC-SMs contribute to the suppression of inherent time-delay estimation (TDE) errors and subsequently improving the tracking performance. All of the above existing MC-SMs have linear sliding variables for achieving asymptotic stability in a simple manner [17], [18]. However, linear sliding variables are disadvantageous in that the corresponding control effort becomes insensitive to tracking errors as the joint angles approach the reference target values. Generally, this disadvantage is not easily overcome by simply increasing gains because high gains for strong attractivity, or fast convergence, may not be allowed to prevent undesirable side effects, such as chattering and noise amplification. In other words, gain tuning has its limitation for the purpose of good tracking performance.

To strengthen the attractivity efficiently and hence control robot manipulators precisely, TDCs with nonsingular terminal sliding-mode (NTSM) have been developed [19]–[21], which is based on nonlinear sliding variables and herein termed model-free controls with NTSM (MC-NTSMs). With NTSM, MC-NTSMs have strong attractivity when the joint angles are close to the reference target values, and hence they provide fast convergence even within the finite time horizon of the prescribed size, or the so-called finite-time convergence. As nonlinear sliding variables provide the effect of high gain controls around reference target values, any undesirable side effects arising from high gains can be avoided. Thus far, several modified versions of MC-NTSMs have been developed with continuous NTSM [22], continuous nonsingular fast terminal sliding mode [23], and fractional-order NTSM [24]. Additionally, for more flexible response to changing conditions, adaptive controls based on NTSM have also been suggested without employing TDC [25]–[28]. Their adaptive gains are not practical because monotonic one-way adaptation with saturation is only considered for the initial transient response.

Therefore, the aforementioned existing MC-NTSMs and relevant controls have much room for improvement regarding tracking performance:

- As mentioned earlier, the existing MC-NTSMs employ the fixed control gains and some adaptive controls based on NTSM adopt adaptive gains that are difficult to implement. Fixed gains are often not flexible in terms of tracking performance improvement and noise suppression. Proper gains should be applied at the right times by adjusting their magnitudes in order to provide good performance constantly without undesirable side effects. It would be meaningful to adjust the control gains over time to consider multiple criteria.
- The inherent TDE errors of existing MC-NTSMs are assumed to be upper bounded [29]–[33]. However, when the friction force becomes opposite in sign due to the directional change of motion or a reference trajectory has non-smooth points, TDE errors may be large, potentially affecting the involving TDC in a negative manner, with consequent poor tracking errors [34], [35]. For this reason, the upper bounds of the TDE errors are generally set to be sufficiently large, and the switching gains adopted in MC-NTSMs are accordingly taken to be large even though chattering may occur. It would be desirable to adjust the switching gains appropriately according to the TDE errors.
- As in the control gains, the nonlinear sliding variables of the existing MC-NTSMs have an inherent trade-off between tracking performance and noise effects arising from the derivative of tracking errors. It would be thus meaningful to develop a method for overcoming such an underlying trade-off.

Several research have been conducted considering the three issues mentioned above [36], [37]. This paper proposes an AMC-NTSM for achieving high precision and fast response, and applies it to robot manipulators. A solution to each issue above is provided in the proposed AMC-NTSM as follows:

- The control gains of the proposed AMC-NTSM increase when the sliding variable stays far away from the sliding manifold. On the contrary, the control gains decrease when the sliding variable remains near the sliding manifold. Such adaptive control gains are very helpful for improving tracking performance while mitigating the effect of noise.
- The switching gains of the proposed AMC-NTSM are adjusted in proportion to the magnitude of acceleration that is associated with the upper bound of TDE errors. Such gain adjustment is effective for increases in TDE errors due to large acceleration. Thus, they can appropriately suppress the TDE errors of any magnitude while reducing chattering.
- Sliding variables are directly reflected on the proposed AMC-NTSM to support fast convergence with moderate gains while achieving uniform ultimate boundedness of tracking errors. This plays a role in resolving the aforementioned trade-off arising from nonlinear sliding variables of existing MC-NTSMs.

In summary, the proposed AMC-NTSM is aimed at reinforcing an existing MC-NTSM with adaptive schemes, flexible TDE error suppression, and responsive practical control in order to achieve better tracking performance while reducing undesirable side effects.

The remainder of this paper is organized as follows: in Section II, a conventional TDC and an MC-NTSM are briefly introduced. The proposed AMC-NTSM isg presented in Section III. Section IV describes simulations carried out with a two-link robot manipulator. The application of the proposed AMC-NTSM to real robot manipulators is described in Section V. We conclude with a brief summarization of the results of this paper in Section VI.

II. TIME-DELAY CONTROL & MODEL-FREE CONTROL WITH NONSINGULAR TERMINAL SLIDING-MODE

A. TIME-DELAY CONTROL

The dynamics of a n-link rigid robotic manipulator [38] can be described as

$$\mathbf{M}(\mathbf{q}_t)\ddot{\mathbf{q}}_t + \mathbf{C}(\mathbf{q}_t, \dot{\mathbf{q}}_t)\dot{\mathbf{q}}_t + \mathbf{g}(\mathbf{q}_t) + \mathbf{f}(\dot{\mathbf{q}}_t) = \boldsymbol{\tau}_t - \boldsymbol{\tau}_{d,t} \quad (1)$$

where $\mathbf{q}_t$, $\dot{\mathbf{q}}_t$, and $\ddot{\mathbf{q}}_t \in \Re^n$ are the angle, angular velocity, and angular acceleration of the joints, respectively; $\mathbf{M}(\mathbf{q}_t) \in \Re^{n\times n}$ is the symmetric positive definite inertia matrix; $\mathbf{C}(\mathbf{q}_t, \dot{\mathbf{q}}_t) \in \Re^n$ is the Coriolis matrix; $\mathbf{g}(\mathbf{q}_t) \in \Re^n$ is the gravity force; $\mathbf{f}(\dot{\mathbf{q}}_t) \in \Re^n$ is the friction force, and $\boldsymbol{\tau}_{d,t} \in \Re^n$; and $\boldsymbol{\tau}_t \in \Re^n$ are the external disturbance and the control input torque, respectively. It is reasonably assumed that $\|\boldsymbol{\tau}_{d,t}\|$ and $||\mathbf{M}(\mathbf{q}_t)||$ are bounded [39]. Any norm can be used if not specified. Only the ∞ norm is specified if necessary.

Adding $\tau_{d,t}$ to both sides of (1), we have

$$\boldsymbol{\tau}_t = \mathbf{C}(\mathbf{q}_t, \dot{\mathbf{q}}_t)\dot{\mathbf{q}}_t + \mathbf{g}(\mathbf{q}_t) + \mathbf{f}(\dot{\mathbf{q}}_t) + \boldsymbol{\tau}_{d,t} + [\mathbf{M}(\mathbf{q}_t) - \bar{\mathbf{M}}]\ddot{\mathbf{q}}_t + \bar{\mathbf{M}}\ddot{\mathbf{q}}_t, \quad (2)$$

where $\bar{\mathbf{M}} = \mathrm{diag}(\bar{M}_1, \bar{M}_2, \cdots, \bar{M}_n) \in \Re^{n\times n}$ is a positive matrix to be determined in the next subsection. Multiplying both sides of (1) by $\mathbf{M}^{-1}(\mathbf{q}_t)$ and representing (2) in a compact and simple form yield

$$\ddot{\mathbf{q}}_t = \mathbf{N}_t + \bar{\mathbf{M}}^{-1}\boldsymbol{\tau}_t \quad (3)$$

where $\mathbf{N}_t$ is given by

$$\mathbf{N}_t = -\bar{\mathbf{M}}^{-1}\left\{\mathbf{C}(\mathbf{q}_t, \dot{\mathbf{q}}_t)\dot{\mathbf{q}}_t + \mathbf{g}(\mathbf{q}_t) + \mathbf{f}(\dot{\mathbf{q}}_t) + \boldsymbol{\tau}_{d,t}\right\} - \bar{\mathbf{M}}^{-1}\left\{[\mathbf{M}(\mathbf{q}_t) - \bar{\mathbf{M}}]\ddot{\mathbf{q}}_t\right\}.$$

Since $\mathbf{N}_t$ in (3) is not available due to unknown external disturbances at time t, its estimate $\hat{\mathbf{N}}_t$ is determined in the following simple manner:

$$\hat{\mathbf{N}}_t \triangleq \mathbf{N}_{t-L} = \ddot{\mathbf{q}}_{t-L} - \bar{\mathbf{M}}^{-1}\boldsymbol{\tau}_{t-L} \quad (4)$$

where L is a sufficiently small sampling period and $\hat{\mathbf{N}}_t = (\hat{N}_{1,t}, \hat{N}_{2,t}, \cdots, \hat{N}_{n,t}) \in \Re^n$. It is noted that $\hat{\mathbf{N}}_t$ is simply a one-sample delayed measurement of $\mathbf{N}_t$ [40]. From (4), the conventional TDC $\bar{\boldsymbol{\tau}}_t^{\mathrm{TDC}}$ can be represented in the following form [41]

$$\bar{\boldsymbol{\tau}}_t^{\mathrm{TDC}} = -\bar{\mathbf{M}}\ddot{\mathbf{q}}_{t-L} + \bar{\boldsymbol{\tau}}_{t-L}^{\mathrm{TDC}} + \bar{\mathbf{M}}(\ddot{\mathbf{q}}_{d,t} + \mathbf{K}_d\dot{\mathbf{e}}_t + \mathbf{K}_p\mathbf{e}_t), \quad (5)$$

where $\mathbf{e}_t = \mathbf{q}_{d,t} - \mathbf{q}_t \in \Re^n$ is the tracking error, and $\mathbf{K}_d = \mathrm{diag}(K_{d1}, K_{d2}, \cdots, K_{dn}) \in \Re^{n\times n}$ and $\mathbf{K}_p = \mathrm{diag}(K_{p1}, K_{p2}, \cdots, K_{pn}) \in \Re^{n\times n}$ are positive gains for pole assignment.

Replacing τ_t in (3) with $\bar{\boldsymbol{\tau}}_t^{\mathrm{TDC}}$ in (5), we can obtain the error dynamics as

$$\ddot{\mathbf{e}}_t + \mathbf{K}_d\dot{\mathbf{e}}_t + \mathbf{K}_p\mathbf{e}_t + \mathbf{E}_t = 0 \quad (6)$$

where $\mathbf{E}_t = \mathbf{N}_t - \hat{\mathbf{N}}_t \in \Re^n$ is called the TDE errors and known to be bounded as follows [19], [33]:

$$|E_{i,t}| \le E_i^* \quad (7)$$

for a positive constant E_i^* under some conditions. In this study, the upper bounds E_i^* are parameterized in terms of acceleration and then TDE errors of any magnitude can be suppressed with the proposed AMC-NTSM. Details are provided in Appendix A.

B. MODEL-FREE CONTROL WITH NONSINGULAR TERMINAL SLIDING-MODE

To improve the error convergence rate, we employ the nonsingular terminal sliding variable expressed in the following form [20]:

$$\mathbf{s}_t = \mathbf{e}_t + \mathbf{K}_s(\dot{\mathbf{e}}_t)^{\frac{p}{q}}, \quad 1 < \frac{p}{q} < 2 \quad (8)$$

for positive odd integers p and q, and a constant matrix $\mathbf{K}_s$ to be determined for adjusting the convergence rate. $\mathbf{s}_t$ and $\mathbf{K}_s$ in (8) have n scalar elements, or $\mathbf{s}_t = (s_{1,t}, s_{2,t}, \cdots, s_{n,t})^T \in \Re^n$ and $\mathbf{K}_s = \mathrm{diag}(K_{s1}, K_{s2}, \cdots, K_{sn}) \in \Re^{n\times n}$.

From (8), the MC-NTSM $\bar{\boldsymbol{\tau}}_t^{\mathrm{N}}$ is given as follows [19]:

$$\bar{\boldsymbol{\tau}}_t^{\mathrm{N}} = -\bar{\mathbf{M}}\ddot{\mathbf{q}}_{t-L} + \bar{\boldsymbol{\tau}}_{t-L}^{\mathrm{N}} + \bar{\mathbf{M}}\Big[\ddot{\mathbf{q}}_{d,t} + \frac{q}{p}\mathbf{K}_s^{-1}(\dot{\mathbf{e}}_t)^{2-\frac{p}{q}} + \bar{\mathbf{K}}_{sw}\mathrm{sgn}(\mathbf{s}_t)\Big] \quad (9)$$

where $\bar{\mathbf{K}}_{sw} = \mathrm{diag}(\bar{K}_{sw,1}, \bar{K}_{sw,2}, \cdots, \bar{K}_{sw,n}) \in \Re^{n\times n}$ is a design parameter with positive elements and $\mathrm{sgn}(\mathbf{s}_t) = [\mathrm{sgn}(s_{1,t}), \mathrm{sgn}(s_{2,t}), \cdots, \mathrm{sgn}(s_{n,t})] \in \Re^n$ is defined as

$$\mathrm{sgn}(s_{i,t}) = \begin{cases} 1 & \text{if} \quad s_{i,t} \ge 0 \\ -1 & \text{if} \quad s_{i,t} < 0 \end{cases} \quad (10)$$

Three gains, $\bar{\mathbf{M}}$, $\mathbf{K}_s$, and $\bar{\mathbf{K}}_{sw}$ in (9) are termed control, sliding, and switching gains, respectively, throughout this paper. The control gain $\bar{\mathbf{M}}$ in (9) is multiplied by the acceleration computed by the numerical differentiation. For this reason, if a large control gain $\bar{\mathbf{M}}$ is employed to improve tracking performance, the effects of noise may be amplified. In contrast, if a small control gain $\bar{\mathbf{M}}$ is selected, the effects of noise will be reduced, but the tracking performance may be degraded. In this regard, the control gains need to be tactically adjusted over time considering multi-criteria. Similarly, (9) observed that if the sliding gain $\mathbf{K}_s$ in (8) is increased to achieve a faster convergence rate, the feedback gain with respect to the time derivative of the tracking error is reduced and hence the transient response may be poor. High switching gains $\bar{\mathbf{K}}_{sw}$ for improving robust performance also cause undesirable side effects such as chattering.

In the following section, the abovementioned design control and switching gains, and compensation for large sliding gains are discussed.

III. ADAPTIVE MODEL-FREE CONTROL WITH NONSINGULAR TERMINAL SLIDING-MODE

We propose an adaptive model-free control with nonsingular terminal sliding-mode (AMC-NTSM) as follows:

$$\boldsymbol{\tau}_t = \hat{\mathbf{M}}_t[-\ddot{\mathbf{q}}_{t-L} + \hat{\mathbf{M}}_t^{-1}\boldsymbol{\tau}_{t-L}]$$

$$+\hat{\mathbf{M}}_t[\ddot{\mathbf{q}}_{d,t} + \frac{q}{p}\mathbf{K}_s^{-1}(\dot{\mathbf{e}}_t)^{2-\frac{p}{q}} + \beta\mathbf{s}_t + \hat{\mathbf{K}}_{sw,t}\mathrm{sgn}(\mathbf{s}_t)]$$
$$= \hat{\mathbf{M}}_t\mathbf{\Psi}_t + \boldsymbol{\tau}_{t-L} \tag{11}$$

where $\mathbf{\Psi}_t = (\Psi_{1,t}, \Psi_{2,t}, \cdots, \Psi_{n,t}) \in \Re^n$ is given by

$$\mathbf{\Psi}_t = -\ddot{\mathbf{q}}_{t-L} + \ddot{\mathbf{q}}_{d,t} + \frac{q}{p}\mathbf{K}_s^{-1}\left(\dot{\mathbf{e}}_t\right)^{2-\frac{p}{q}} + \beta\mathbf{s}_t + \hat{\mathbf{K}}_{sw,t}\mathrm{sgn}(\mathbf{s}_t)$$

and $\hat{\mathbf{K}}_{sw,t} = \mathrm{diag}\left(\hat{K}_{sw,1,t}, \hat{K}_{sw,2,t}, \cdots, \hat{K}_{sw,n,t}\right) \in \Re^{n\times n}$ is defined as

$$\hat{K}_{sw,i,t} = \bar{K}_{0i} + \bar{K}_{1i}||\ddot{\mathbf{q}}_t|| \tag{12}$$

for positive design parameters $\bar{K}_{0i}$ and $\bar{K}_{1i}$ to be determined carefully for suppressing the TDE errors and simultaneously not being sensitive to acceleration. Details on the selection of $\bar{K}_{0i}$ and $\bar{K}_{1i}$ are shown in Appendix B. As mentioned in the previous section, the sliding variable $\mathbf{s}_t$ in (11) plays a key role in producing more responsive control efforts regardless of large $\mathbf{K}_s$ or small $\mathbf{K}_s^{-1}$. β and $\hat{M}_t$ contribute towards guaranteeing fast convergence and suppression of large TDE errors effectively.

In (11), the time-varying control gain $\hat{\mathbf{M}}_t$ is automatically tuned as follows:

$$\hat{M}_{i,t} = \begin{cases} \bar{M}_i\left(1 + \phi_i\hat{\omega}_{i,t}\right) & \text{if} \quad s_{i,t}\Psi_{i,t} > 0 \\ \bar{M}_i & \text{if} \quad s_{i,t}\Psi_{i,t} \le 0 \end{cases} \tag{13}$$

where $\bar{M}_i$ and ϕ_i are positive constants and $\hat{\omega}_{i,t}$ is a time-varying positive gain determined by the following adaptive law:

$$\dot{\hat{\omega}}_{i,t} = \begin{cases} -\alpha_i\gamma_i(\frac{1}{|s_{i,t}|} + \rho_i) & \text{if } \hat{\omega}_{i,t} = \bar{\omega}_i^* \\ \alpha_i(\gamma_i^{-1})^{\theta_t}(|s_{i,t}|^{\theta_t} + \frac{\rho_i}{\tilde{\omega}_{i,t}})\theta_t & \text{if } 0 < \hat{\omega}_{i,t} < \bar{\omega}_i^* \\ \frac{\alpha_i}{\gamma_i}(|s_{i,t}| + \frac{\rho_i}{\tilde{\omega}_{i,t}}) & \text{if } \hat{\omega}_{i,t} = 0 \text{ or } s_{i,t} = 0 \end{cases} \tag{14}$$

for $\tilde{\omega} = \bar{\omega}^* - \hat{\omega}$ and $\theta_t = \mathrm{sgn}(||\mathbf{s}_t||_\infty - \varepsilon)$ and positive design parameters α_i, γ_i, ρ_i, and ε where $\|\cdot\|_\infty$ is the ∞ norm of a vector. It is noted that $\bar{M}_i$ in (13) can be considered as a lower bound of $\hat{M}_{i,t}$. A sufficiently small ε is selected such that the tracking error is tolerable.

As shown in (14), the time-varying gain $\hat{w}_{i,t}$ is strongly affected by ε. The front term in (14) can easily adjust the rate of increase or decrease of the time-varying gain $\hat{w}_{i,t}$ by setting $\frac{\alpha_i}{\gamma_i}$ for $||\mathbf{s}_t||_\infty \ge \varepsilon$ and $-\alpha_i\gamma_i$ for $||\mathbf{s}_t||_\infty < \varepsilon$, independently. The working principle of the proposed AMC-NTSM for two cases, $||\mathbf{s}_t||_\infty \ge \varepsilon$ and $||\mathbf{s}_t||_\infty < \varepsilon$, can be described as follows.

- In case of $||\mathbf{s}_t||_\infty \ge \varepsilon$
  The control gain $\hat{M}_{i,t}$ increases until $||\mathbf{s}_t||_\infty$ reaches ε. As $\dot{\hat{w}}_{i,t}$ in (14) is linearly related to $|s_{i,t}|$, the large sliding variable will be dominant on the adaptive law and then provide strong attractiveness to the sliding manifold.
  However, as the sliding variable approaches the small vicinity of the sliding manifold, or the set $||\mathbf{s}_t||_\infty < \varepsilon$, the convergence rate declines because $|s_{i,t}|$ in (14) becomes small. To solve this problem, we employ an additional term that compensates for small $|s_{i,t}|$ and hence quickly drives the sliding variable to the set $||\mathbf{s}_t||_\infty < \varepsilon$.
- In case of $||\mathbf{s}_t||_\infty < \varepsilon$
  As the sliding variable $\mathbf{s}_t$ enters the set $||\mathbf{s}_t||_\infty < \varepsilon$ and then θ_t becomes negative, the control gain $\hat{M}_{i,t}$ is reduced to avoid undesirable side effects generated by excessively high control gains. In addition, $|s_{i,t}|^{-1}$ in (14) is inversely proportional to the magnitude of the sliding variable, which provides strong attractiveness near the sliding manifold.

It is noted that while a disturbance observer (DOB) based control (DOBC) [11], [12] is based on the frequency-domain and only applicable to the minimum phase systems, TDC employed in this paper is computed directly in the time-domain by using time-delayed measurements. For one concrete example, abrupt disturbances over short time intervals can be more easily handled by the proposed AMC-NTSM than by DOBC.

To sum up, the AMC-NTSM uses the adaptive control gain $\hat{\mathbf{M}}_t$ to reduce the magnitude of the TDE error caused by the fixed control gain $\bar{\mathbf{M}}_t$ of the TDC controller. In addition, the generated TDE error is appropriately suppressed using the switching gain $\hat{K}_{s\omega,t}$. Chattering is also reduced by adopting small switching gains after convergence.

The stability of the proposed AMC-NTSM is discussed in Appendix B. Its effectiveness will be illustrated in the next sections.

IV. SIMULATION

A. SIMULATION SETUP

A simulation was performed to illustrate the effectiveness of the proposed AMC-NTSM (11) with a two-link planar manipulator [42] described as

$$\mathbf{M}(\mathbf{q}_t)_{11} = l_2^2m_2 + 2l_1l_2m_2c_2 + l_1^2(m_1+m_2)$$
$$\mathbf{M}(\mathbf{q}_t)_{12} = \mathbf{M}(\mathbf{q}_t)_{21} = l_2^2m_2 + l_1l_2m_2c_2,\ \mathbf{M}(\mathbf{q}_t)_{22} = l_2^2m_2$$
$$\mathbf{C}(\mathbf{q}_t, \dot{\mathbf{q}}_t)\dot{\mathbf{q}}_t = \begin{bmatrix} -m_2l_1l_2s_2\dot{q}_{2,t}^2 - 2m_2l_1l_2s_2\dot{q}_{1,t}\dot{q}_{2,t} \\ m_2l_1l_2s_2\dot{q}_{2,t}^2 \end{bmatrix}$$
$$\mathbf{G}(\mathbf{q}_t) = \begin{bmatrix} m_2l_2gc_{12} + (m_1+m_2)l_1gc_1 \\ m_2l_2gc_{12} \end{bmatrix}$$
$$\mathbf{F}(\dot{\mathbf{q}}_t) = \begin{bmatrix} \lambda_{11}\dot{q}_{1,t} + \lambda_{12}\mathrm{sgn}(\dot{q}_{1,t}) \\ \lambda_{21}\dot{q}_{2,t} + \lambda_{22}\mathrm{sgn}(\dot{q}_{2,t}) \end{bmatrix}$$

where relevant physical parameters are shown in Table 1; $q_{i,t}$ is the angle for the joint i, and s_i, c_i, and c_{ij} are defined by $\sin\left(q_{i,t}\right)$, $\cos\left(q_{i,t}\right)$, and $\cos\left(q_{i,t} + q_{j,t}\right)$, respectively.

Design parameters of the proposed AMC-NTSM were selected as follows: $\mathbf{K}_s = \mathrm{diag}(0.9, 0.9)$, $\beta = 2000$, $L = 0.25$ ms, $p = 5$, $q = 3$, $\bar{M}_1 = 0.08$, $\bar{M}_2 = 0.04$, $\phi_1 = \phi_2 = 5$, $\alpha_1 = \alpha_2 = 100$, $\gamma_1 = \gamma_2 = 100$, $\rho_1 = \rho_2 = 0.1$,

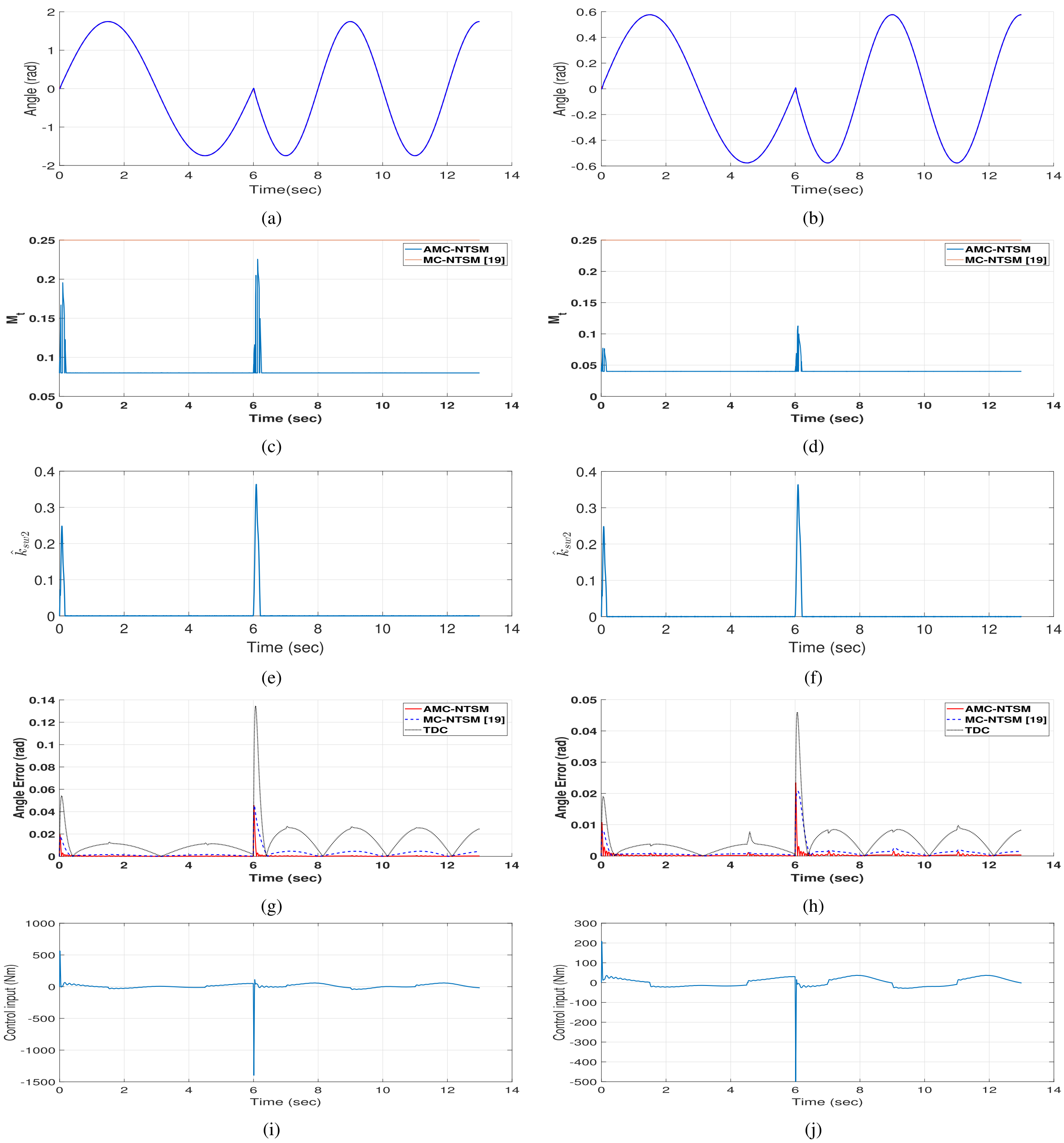

FIGURE 1. Trajectories of the reference angles: (a) 1st joint. (b) 2nd joint. Adaptive control gains of the proposed AMC-NTSM: (c) 1st joint. (d) 2nd joint. Adaptive switching gains of the proposed AMC-NTSM: (e) 1st joint. (f) 2nd joint. Comparison of tracking errors generated from TDC (dotted line), MC-NTSM (dashed line), the proposed AMC-NTSM (solid line): (g) 1st joint. (h) 2nd joint. Control input (Torque) of AMC-NTSM: (i) 1st joint. (j) 2nd joint.

$\bar{\omega}_1^* = \bar{\omega}_2^* = 2$, $K_{01} = K_{02} = 0.01$, $K_{11} = K_{12} = 0.005$, and $\varepsilon = 0.03$.

B. SIMULATION DESCRIPTION

The practical effectiveness of the proposed AMC-NTSM (11) is shown through comparisons with TDC [41] in (5) and the existing MC-NTSM [19] in (9). The control objective is to ensure that the angles of joints 1 and 2 follow the reference trajectories that include low and high frequency components and have non-differential points as shown in Fig. 1(a) and (b). All control schemes adopted for comparison were first designed to be properly tuned in the low frequency component and then they were applied to the given reference trajectories in order to test their adaptiveness and robustness to changing conditions. The smaller the sampling time, the better the performance of the proposed control scheme. In this study, the sampling time was set to 0.25 ms for both the simulation and experiments.

TABLE 1. Physical parameters of the robot manipulator.

Joint	Mass m (kg)	Length l (mm)	Gravity g (m/s^2)	Friction λ $(N \cdot m)$
1	1	1000	9.81	5
2	1	800		

TABLE 2. RMS values of tracking errors (simulation).

Control strategies	1st joint (rad)	2nd joint (rad)
TDC [41]	2.01×10^{-2}	0.68×10^{-2}
MC-NTSM [19]	0.51×10^{-2}	0.28×10^{-2}
The proposed AMC-NTSM	0.25×10^{-2}	0.12×10^{-2}

TABLE 3. RMS values of tracking errors with square trajectories (simulation).

Control strategies	1st joint (rad)	2nd joint (rad)
MC-NTSM [12]	1.805×10^{-1}	1.913×10^{-1}
The proposed AMC-NTSM with a nominal model	1.496×10^{-1}	1.488×10^{-1}
The proposed AMC-NTSM with an uncertain system	1.50×10^{-1}	1.504×10^{-1}

C. SIMULATION RESULTS

Fig. 1(c) and (d) show the control gains computed from the adaptive law (13) of the proposed AMC-NTSM. For a large amount of time, the control gains have low bounded values, or large control gains are applied only when necessary in order to avoid undesirable side effects such as chattering and input oscillation. In particular, when directional change of motion occurs, or the friction force becomes opposite in sign, large controls are applied temporarily. Fig. 1(e) and (f) show that as in the control gains, the switching gains in Fig. 1 (c) and (d) of the proposed AMC-NTSM are enlarged only when necessary. As mentioned earlier, they are dependent on the acceleration and effective in suppressing TDE errors. Fig. 1(g) and (h) show tracking errors of the proposed AMC-NTSM compared with those of TDC (5) and MC-NTSM (9). The existing TDC (5) appears to produce the worst, or largest tracking error. The existing MC-NTSM [19] has larger tracking error than the proposed AMC-NTSM because the sliding gains $\mathbf{K}_s$ in (9) cannot be increased much for improving the tracking performance as a result of their inverse effect on the control effort. This is why sliding variables are directly added to the proposed AMC-NTSM in order to obtain more responsive control. With the help of adaptive gains, TDE error suppression, and responsive control, the proposed AMC-NTSM exhibited a good tracking performance. Quantitatively, the measured root-mean-square (RMS) errors are summarized in Table 2 and 3. Fig. 1(i) and(j) show the control input of each joint.

V. EXPERIMENT

A. EXPERIMENTAL SETUP

An Indy7 robot manipulator, as shown in Fig. 2, was employed to carry out the experiments. This robot manipulator was controlled by a PC-based controller running on a real-time EtherCAT Master implemented on Xenomi and IndyFramework 2.0. As measurement devices, encoders are adopted to measure joint angles, with a resolution of 16 bit (65536 counts/turn). The gear ratio was set to be 1:121 for the 1st joint to the 3rd joint, and 1:101 for the 4th joint to the 5th joint. The hardware configuration is given in Table 4.

(a) (b)

FIGURE 2. A Neuromeka Indy7 robot manipulator: (a) Without, (b) With payload.

For comparison, the existing model-free control, or MC-NTSM [19], was employed. The control parameters of the proposed AMC-NTSM were set to $L = 0.25$ ms, $p = 5$, $q = 3$, $\bar{M} = \text{diag}(0.3, 0.2, 0.1, 0.08, 0.07, 0.06)$ kg·m^2, $K_s = \text{diag}(1.5, 0.75, 2.0, 10.0, 7.5, 7.5)$, $\beta = \text{diag}(15, 20, 20, 20, 20, 20)$, $\bar{K}_{0i} = \text{diag}(0.001, 0.001, 0.001, 0.001, 0.001, 0.001)$, $\bar{K}_{1i} = \text{diag}(0.008, 0.008, 0.01, 0.05, 0.05, 0.05)$, $\varepsilon = 0.03$, $\alpha = 2$, $\gamma = 10$, $\rho = 0.1$, $\bar{\omega}^* = 2$, and $\phi = 1000$. Regarding the parameters of MC-NTSM, the same as in [19] were selected. The initial condition of both controls were set to $\mathbf{q}_0 = (0,0)$.

B. EXPERIMENTAL DESCRIPTION

To ensure good performance of the proposed AMC-NTSM in real systems, the model-free control [19] was compared through experiments. The control objective was to achieve robust tracking performance against external disturbances due to the payload. The payload affects the Indy7 robot manipulator according to the position and acceleration of joints. The reference and real angle trajectories are shown in in Fig. 3(a). To compute second derivative of displacement, proper filtering would be helpful for numerical accuracy.

C. EXPERIMENTAL RESULTS

The experimental results of the proposed AMC-NTSM are shown in Fig. 3. The reference was provided by its generator in the Indy7 robot manipulator such that all joints were moved to pass through 4 waypoints. The resulting tracking performance of each joint is shown in Fig. 3(a). The time-varying control gains (13) are shown in Fig. 3(c). When the direction is changed, $\mathbf{M}_t$ increases for fast convergence are shown in Fig. 3(c) and (f). Fig. 3(d) shows the tracking errors of two controls: MC-NTSM and the proposed AMC-NTSM. As in simulation results, the proposed AMC-NTSM provides outstanding nominal tracking ability compared with MC-NTSM, especially in case of directional change of motion, or

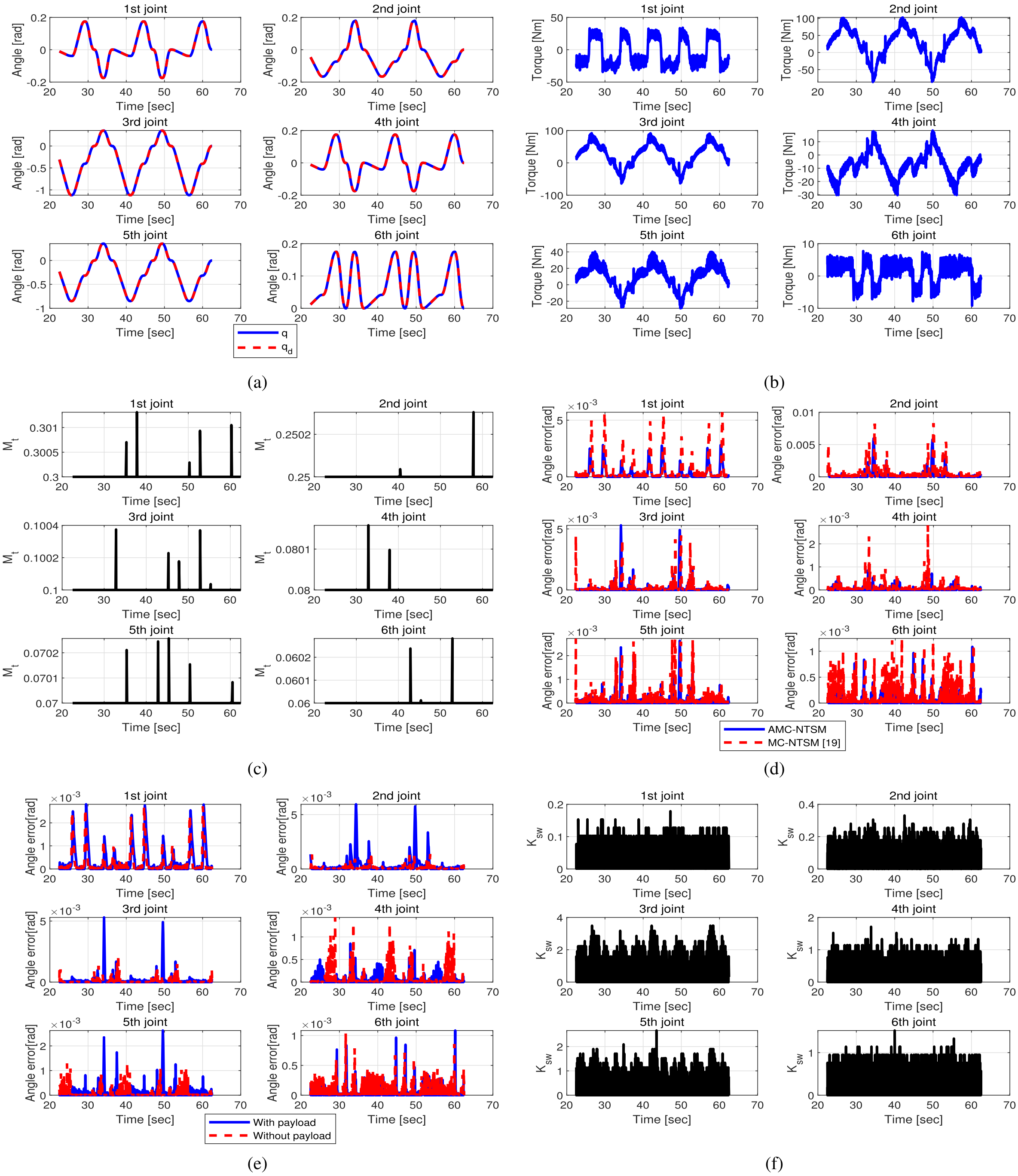

FIGURE 3. Experiment results with payload of 5 kg. (a) The desired and real angle trajectories. (b) Control input (torque) of each joint. (c) Adaptive control gains of the proposed AMC-NTSM. (d) Comparison of the tracking errors of MC-NTSM (red dashed line), and the proposed AMC-NTSM (blue solid line): (without payload). (e) Comparison of the robust tracking error with payload. (f) Adaptive switching gains of the proposed AMC-NTSM.

TABLE 4. Hardware configuration.

DOF	Payload (kg)	Joint motion Range (rad)	Max. joint velocity (rad/s)	Sampling time (ms)
6 (Joints are all revolute)	7	1st to 5th joints: -3.0543 to 3.0543 6th joint: -3.7525 to 3.7525	1st to 3rd joints: 2.6180 4th to 6th joints: 3.1416	0.25

TABLE 5. RMS values of tracking errors (experiment).

Control strategies	1st joint (rad)	2nd joint (rad)	3rd joint (rad)	4th joint (rad)	5th joint (rad)	6th joint (rad)
MC-NTSM [19] with payload	12.0×10^{-4}	14.0×10^{-4}	5.4756×10^{-4}	1.9115×10^{-4}	3.9654×10^{-4}	2.6364×10^{-4}
The proposed AMC-NTSM with payload	6.7074×10^{-4}	8.7964×10^{-4}	5.5104×10^{-4}	0.94391×10^{-4}	2.8513×10^{-4}	1.1693×10^{-4}
The proposed AMC-NTSM without payload	5.9563×10^{-4}	2.4033×10^{-4}	2.1623×10^{-4}	2.0526×10^{-4}	2.0496×10^{-4}	1.3995×10^{-4}

opposite sign of the friction force. For quantitative tracking error analysis, the RMS values of tracking errors are summarized in Table 5. Since the lower part of the robot manipulator is more loaded, it has a relatively large RMS tracking error. Overall, the tracking error of the AMC-NTSM was almost half that of the existing MC-NTSM [19].

To evaluate the robust tracking performance, we tuned the parameters of the controller without payload, and then applied them with a payload of 5 kg. Real experiments were also performed with a payload of 5 kg, corresponding to about 70% of the maximum load. A payload can be considered as an external disturbance. The results are shown in Fig. 3(e). The RMS values of the resulting tracking errors are summarized in Table 5. Despite payload uncertainty, the robust and nominal tracking performances did not differ much. In most joints, the RMS value of the tracking errors with payload was slightly larger than that without payload. In addition, the RMS of the proposed control scheme can be observed to be improved by at least 46% compared with that of other controllers.

VI. CONCLUSION

This work proposed an adaptive model-free control with nonsingular terminal sliding-mode (AMC-NTSM), and its effectiveness was evaluated through simulations and experiments with robot manipulators. The transient and steady-state tracking performances of the proposed AMC-NTSM could be remarkably improved due to the synergetic effects of adaptive (control and switching) gains and sliding variables used for control inputs. Moreover, undesirable side effects on chattering and noise amplification could be suppressed as much as possible by reducing gains appropriately at the right times. The experiment result with payload showed that the proposed AMC-NTSM has more robust tracking performance than existing controls.

With simple implementation and good tracking performance, the proposed AMC-NTSM is a potential candidate for replacing existing controls for application to robot manipulators. We also believe that the applications of the proposed AMC-NTSM can be further extended to diverse systems.

APPENDIX A
BOUNDEDNESS OF BLUETIME-DELAY ESTIMATION ERROR

From (3) and (4), the TDE error $\mathbf{E}_t$ can be rewritten as follows:

$$\mathbf{E}_t = \mathbf{N}_t - \hat{\mathbf{N}}_t. \tag{15}$$

Substitute $\mathbf{N}_t$ and $\hat{\mathbf{N}}_t$ into (15), we have

$$\begin{aligned}\mathbf{E}_t = &-\bar{\mathbf{M}}^{-1}\big[\mathbf{C}(\mathbf{q}_t,\dot{\mathbf{q}}_t)\dot{\mathbf{q}}_t - \mathbf{C}(\mathbf{q}_{t-L},\dot{\mathbf{q}}_{t-L})\dot{\mathbf{q}}_{t-L}\big]\\ &-\bar{\mathbf{M}}^{-1}\big[\mathbf{g}(\mathbf{q}_t) - \mathbf{g}(\mathbf{q}_{t-L}) + \mathbf{f}(\dot{\mathbf{q}}_t) - \mathbf{f}(\dot{\mathbf{q}}_{t-L})\big]\\ &-\bar{\mathbf{M}}^{-1}\big[\boldsymbol{\tau}_{d,t} - \boldsymbol{\tau}_{d,t-L}\big]\\ &-\bar{\mathbf{M}}^{-1}\big\{[\mathbf{M}(\mathbf{q}_t)-\bar{\mathbf{M}}]\ddot{\mathbf{q}}_t - [\mathbf{M}(\mathbf{q}_{t-L}) - \bar{\mathbf{M}}]\ddot{\mathbf{q}}_{t-L}\big\}.\end{aligned} \tag{16}$$

Then, we have

$$\begin{aligned}\mathbf{E}_t = &\ \boldsymbol{\nu}_{\mathrm{con},t} + \boldsymbol{\nu}_{\mathrm{dis},t} - \bar{\mathbf{M}}^{-1}\big\{[\mathbf{M}(\mathbf{q}_t) - \bar{\mathbf{M}}]\ddot{\mathbf{q}}_t\big\}\\ &+\bar{\mathbf{M}}^{-1}\big\{[\mathbf{M}(\mathbf{q}_{t-L}) - \bar{\mathbf{M}}]\ddot{\mathbf{q}}_{t-L}\big\}\\ = &\ \boldsymbol{\nu}_{\mathrm{con},t} + \boldsymbol{\nu}_{\mathrm{dis},t} - \bar{\mathbf{M}}^{-1}\big\{[\mathbf{M}(\mathbf{q}_t) - \bar{\mathbf{M}}]\ddot{\mathbf{q}}_t\big\}\\ &+\bar{\mathbf{M}}^{-1}\big\{[\mathbf{M}(\mathbf{q}_{t-L}) - \bar{\mathbf{M}}][\ddot{\mathbf{q}}_t - \bar{\mathbf{z}}_t]\big\}\end{aligned} \tag{17}$$

where $\boldsymbol{\nu}_{\mathrm{con},t} = -\bar{\mathbf{M}}^{-1}\big[\mathbf{C}(\mathbf{q}_t,\dot{\mathbf{q}}_t)\dot{\mathbf{q}}_t - \mathbf{C}(\mathbf{q}_{t-L},\dot{\mathbf{q}}_{t-L})\dot{\mathbf{q}}_{t-L} + \mathbf{g}(\mathbf{q}_t) - \mathbf{g}(\mathbf{q}_{t-L}) + \boldsymbol{\tau}_{d,t} - \boldsymbol{\tau}_{d,t-L}\big] \in \Re^n$, $\boldsymbol{\nu}_{\mathrm{dis},t} = -\bar{\mathbf{M}}^{-1}\big[\mathbf{f}(\dot{\mathbf{q}}_t)-\mathbf{f}(\dot{\mathbf{q}}_{t-L})\big] \in \Re^n$, and $\bar{\mathbf{z}}_t = \ddot{\mathbf{q}}_t - \ddot{\mathbf{q}}_{t-L} \in \Re^n$. For a sufficiently small L, $\boldsymbol{\nu}_{\mathrm{con},t} + \boldsymbol{\nu}_{\mathrm{dis},t}$ are reasonably bounded as follows:

$$\|\boldsymbol{\nu}_{\mathrm{con},t} + \boldsymbol{\nu}_{\mathrm{dis},t}\| \leq \eta_0 \tag{18}$$

where η_0 is a positive constant [19], [33]. Since $\mathbf{M}(\mathbf{q}_t)$ and $\mathbf{M}(\mathbf{q}_{t-L})$ in (17) are bounded [39], we have

$$\begin{aligned}\|\mathbf{E}_t\| &\leq \eta_0 + \|\bar{\mathbf{M}}^{-1}\big\{[\mathbf{M}(\mathbf{q}_{t-L}) - \bar{\mathbf{M}}]\big\}\bar{\mathbf{z}}_t\|\\ &\quad+\|\bar{\mathbf{M}}^{-1}[\mathbf{M}(\mathbf{q}_t) - \mathbf{M}(\mathbf{q}_{t-L})]\|\|\ddot{\mathbf{q}}_t\|\\ &\leq \bar{\eta}_0 + \bar{\eta}_1\|\ddot{\mathbf{q}}_t\|\end{aligned} \tag{19}$$

where $\bar{\eta}_0$ and $\bar{\eta}_1$ are positive constants satisfying the following inequality:

$$\begin{aligned}\eta_0 + \|\bar{\mathbf{M}}^{-1}\big\{[\mathbf{M}(\mathbf{q}_{t-L}) - \bar{\mathbf{M}}]\big\}\bar{\mathbf{z}}_t\| &\leq \bar{\eta}_0\\ \|\bar{\mathbf{M}}^{-1}[\mathbf{M}(\mathbf{q}_t) - \mathbf{M}(\mathbf{q}_{t-L})]\| &\leq \bar{\eta}_1.\end{aligned}$$

It is noteworthy that $\|\ddot{\mathbf{q}}_t - \ddot{\mathbf{q}}_{t-L}\|$ is reasonably assumed to be bounded [33], [43]. From (19), the TDE error $\|\mathbf{E}_t\|$ can be taken as being bounded by a certain first order function of $\|\ddot{\mathbf{q}}_t\|$.

APPENDIX B
PROOF OF STABILITY

For a proof of the stability of the proposed AMC-NTSM (11), the Lyapunov function, denoted by $V_t \in \Re$, is defined as follows:

$$V_t = \frac{1}{2}\mathbf{s}_t^T\mathbf{s}_t + \frac{1}{2}\sum_{i=1}^{n}\frac{\gamma_i}{\alpha_i}\tilde{\omega}_{i,t}^2, \tag{20}$$

in order to guarantee the finite time convergence of the sliding variables and boundedness of adaptive gains. Then, the time derivative of (20) can be obtained as

$$\begin{aligned}\dot{V}_t &= \mathbf{s}_t^T \dot{\mathbf{s}}_t - \textstyle\sum_{i=1}^{n} \frac{\gamma_i}{\alpha_i}\tilde{\omega}_{i,t}\dot{\hat{\omega}}_{i,t} \\ &= \mathbf{s}_t^T \{\dot{\mathbf{e}}_t + \frac{p}{q}\mathbf{K}_s[\mathrm{diag}(\dot{\mathbf{e}}_t)^{\frac{p}{q}-1}]\ddot{\mathbf{e}}_t\} - \chi_t \end{aligned} \tag{21}$$

where $\chi_t = \sum_{i=1}^{n} \frac{\gamma_i}{\alpha_i}\tilde{\omega}_{i,t}\dot{\hat{\omega}}_{i,t}$ and $\ddot{\mathbf{e}}_t = \ddot{\mathbf{q}}_{d,t} - \ddot{\mathbf{q}}_t \in \Re^n$. Substituting (3) into (21) yields

$$\dot{V}_t = \mathbf{s}_t^T \dot{\mathbf{e}}_t + \mathbf{s}_t^T \boldsymbol{\zeta}_t[\ddot{\mathbf{q}}_{d,t} - \mathbf{N}_t - \bar{\mathbf{M}}^{-1}\boldsymbol{\tau}_t] - \chi_t \tag{22}$$

where $\boldsymbol{\zeta}_t = \frac{p}{q}\mathbf{K}_s[\mathrm{diag}(\dot{\mathbf{e}}_t)^{\frac{p}{q}-1}] = \mathrm{diag}(\zeta_{1,t}, \zeta_{2,t}, \cdots, \zeta_{n,t}) \in \Re^{n\times n}$. Substituting (4) and (11) into (22), it follows that

$$\begin{aligned}\dot{V}_t &= \mathbf{s}_t^T \dot{\mathbf{e}}_t - \chi_t \\ &\quad + \mathbf{s}_t^T \boldsymbol{\zeta}_t[-\mathbf{E}_t + \ddot{\mathbf{q}}_{d,t} - \ddot{\mathbf{q}}_{t-L} - \bar{\mathbf{M}}^{-1}\hat{\mathbf{M}}_t\boldsymbol{\Psi}_t]. \end{aligned} \tag{23}$$

Then we have

$$\begin{aligned}\dot{V}_t &= \mathbf{s}_t^T \dot{\mathbf{e}}_t + \mathbf{s}_t^T \boldsymbol{\zeta}_t[-\mathbf{E}_t - \boldsymbol{\varrho}_t - \bar{\mathbf{M}}^{-1}\hat{\mathbf{M}}_t\boldsymbol{\Psi}_t] \\ &\quad + \mathbf{s}_t^T \boldsymbol{\zeta}_t[\boldsymbol{\Psi}_t - \beta\mathbf{s}_t - \hat{\mathbf{K}}_{sw,t}\mathrm{sgn}(\mathbf{s}_t)] - \chi_t \end{aligned} \tag{24}$$

where $\boldsymbol{\varrho}_t = \frac{q}{p}\mathbf{K}_s^{-1}(\dot{\mathbf{e}}_t)^{2-\frac{p}{q}} \in \Re^n$. The TDE error $\mathbf{E}_t = \mathbf{N}_t - \hat{\mathbf{N}}_t \in \Re^n$ is upper bounded by a certain first order function of the acceleration according to (19) in Appendix A. By eliminating $\dot{\mathbf{e}}_t$ from $\boldsymbol{\zeta}_t\boldsymbol{\varrho}_t$ in (24), we have

$$\begin{aligned}\dot{V}_t &= \mathbf{s}_t^T \boldsymbol{\zeta}_t[-\mathbf{E}_t - \hat{\mathbf{K}}_{sw,t}\mathrm{sgn}(\mathbf{s}_t) - \beta\mathbf{s}_t + (\mathbf{I} - \bar{\mathbf{M}}^{-1}\hat{\mathbf{M}}_t)\boldsymbol{\Psi}_t] \\ &\quad - \chi_t \end{aligned} \tag{25}$$

$$\begin{aligned}&\le \textstyle\sum_{i=1}^{n} |s_{i,t}|\zeta_{i,t}(|E_{i,t}| - \hat{K}_{sw,i,t}) \\ &\quad + \mathbf{s}_t^T \boldsymbol{\zeta}_t[-\beta\mathbf{s}_t + (\mathbf{I} - \bar{\mathbf{M}}^{-1}\hat{\mathbf{M}}_t)\boldsymbol{\Psi}_t] - \chi_t \end{aligned} \tag{26}$$

where p and q are positive odd integers with $1 < \frac{p}{q} < 2$. From (12) and (19), if $\bar{K}_{0i}$ and $\bar{K}_{1i}$ are selected as follows:

$$\bar{\eta}_0 < \bar{K}_{0i}, \quad \bar{\eta}_1 < \bar{K}_{1i} \tag{27}$$

for all $i = 1, 2, \cdots, n$, the inequality (26) can be rewritten as follows:

$$\begin{aligned}\dot{V}_t &\le \mathbf{s}_t^T \boldsymbol{\zeta}_t[-\beta\mathbf{s}_t + (\mathbf{I} - \bar{\mathbf{M}}^{-1}\hat{\mathbf{M}}_t)\boldsymbol{\Psi}_t] - \chi_t \\ &= -\beta \textstyle\sum_{i=1}^{n} \zeta_{i,t}s_{i,t}^2 + \sum_{i=1}^{n} s_{i,t}\Psi_{i,t}\zeta_{i,t}(1 - \bar{M}_i^{-1}\hat{M}_{i,t}) \\ &\quad - \textstyle\sum_{i=1}^{n} \frac{\gamma_i}{\alpha_i}\tilde{\omega}_{i,t}\dot{\hat{\omega}}_{i,t}. \end{aligned} \tag{28}$$

Substituting (14) into (28) yields

$$\begin{aligned}\dot{V}_t &\le -\beta \textstyle\sum_{i=1}^{n} \zeta_{i,t}s_{i,t}^2 + \sum_{i=1}^{n} s_{i,t}\Psi_{i,t}\zeta_{i,t}(1 - \bar{M}_i^{-1}\hat{M}_{i,t}) \\ &\quad - \textstyle\sum_{i=1}^{n} \frac{\gamma_i}{\alpha_i}\tilde{\omega}_{i,t}\alpha_i[(\gamma_i^{-1})^{\theta_t}(|s_{i,t}|^{\theta_t} + \frac{\rho_i}{\tilde{\omega}_{i,t}})]\theta_t. \end{aligned} \tag{29}$$

Since for $\|\mathbf{s}_t\|_\infty \ge \varepsilon$, the second term of (29) is less than or equal to zero, we have

$$\begin{aligned}\dot{V}_t &\le -\beta \textstyle\sum_{i=1}^{n} \zeta_{i,t}s_{i,t}^2 - \sum_{i=1}^{n} \tilde{\omega}_{i,t}(|s_{i,t}| + \frac{\rho_i}{\tilde{\omega}_{i,t}}) \\ &\le -\beta \textstyle\sum_{i=1}^{n} \zeta_{i,t}s_{i,t}^2 - \sum_{i=1}^{n}(\tilde{\omega}_{i,t}|s_{i,t}| + \rho_i) \\ &\le -\textstyle\sum_{i=1}^{n} \rho_i. \end{aligned} \tag{30}$$

It means that all sliding variables enter the set, or $\|\mathbf{s}_t\|_\infty < \varepsilon$ within a finite time. However, the derivative of the Lyapunov function is not guaranteed to be negative or zero inside the set $\|\mathbf{s}_t\|_\infty < \varepsilon$.

Once the sliding variable enters the set, or $\|\mathbf{s}_t\|_\infty < \varepsilon$, the Lyapunov function V_t is upper bounded from (20) as follows:

$$\begin{aligned}\frac{1}{2}\|\mathbf{s}_t\|^2 \le V_t &= \frac{1}{2}\textstyle\sum_{i=1}^{n} s_{i,t}^2 + \frac{1}{2}\sum_{i=1}^{n} \frac{\gamma_i}{\alpha_i}\tilde{\omega}_{i,t}^2 \\ &\le \frac{1}{2}n\varepsilon^2 + \frac{1}{2}\bar{\varepsilon} \end{aligned} \tag{31}$$

where $\bar{\varepsilon}$ is the maximum value of $\sum_{i=1}^{n} \frac{\gamma_i}{\alpha_i}\tilde{\omega}_{i,t}^2$. The inequality (31) can be rewritten as

$$\|\mathbf{s}_t\| \le \sqrt{n\varepsilon^2 + \bar{\varepsilon}} = \nu^*. \tag{32}$$

After the sliding variables enter the set, or $\|\mathbf{s}_t\|_\infty < \varepsilon$, they remain upper bounded by ν^*. Even though the sliding variable enters the set, or $\|s\| < \varepsilon$, it may escape from the set, but it should stay in the set $\|s\| < \nu^*$. This completes the proof.

REFERENCES

[1] L. M. Capisani and A. Ferrara, "Trajectory planning and second-order sliding mode Motion/Interaction control for robot manipulators in unknown environments," *IEEE Trans. Ind. Electron.*, vol. 59, no. 8, pp. 3189–3198, Aug. 2012.

[2] J. L. Meza, V. Santibáñez, R. Soto, and M. A. Llama, "Fuzzy self-tuning PID semiglobal regulator for robot manipulators," *IEEE Trans. Ind. Electron.*, vol. 59, no. 6, pp. 2709–2717, Jun. 2011.

[3] R.-J. Lian, "Intelligent controller for robotic motion control," *IEEE Trans. Ind. Electron.*, vol. 58, no. 11, pp. 5220–5230, Nov. 2011.

[4] J. Lee, P. H. Chang, and R. S. Jamisola, "Relative impedance control for dual-arm robots performing asymmetric bimanual tasks," *IEEE Trans. Ind. Electron.*, vol. 61, no. 7, pp. 3786–3796, Jul. 2014.

[5] A. Dumlu and K. Erenturk, "Trajectory tracking control for a 3-DOF parallel manipulator using fractional-order $PI^{\lambda}D^{\mu}$ control," *IEEE Trans. Ind. Electron.*, vol. 61, no. 7, pp. 3417–3426, Jul. 2014.

[6] V. I. Utkin and A. S. Poznyak, "Adaptive sliding mode control with application to super-twist algorithm: Equivalent control method," *Automatica*, vol. 49, no. 1, pp. 39–47, Jan. 2013.

[7] L. Chen, H. Wang, Y. Huang, Z. Ping, M. Yu, X. Zheng, M. Ye, and Y. Hu, "Robust hierarchical sliding mode control of a two-wheeled self-balancing vehicle using perturbation estimation," *Mech. Syst. Signal Process.*, vol. 139, May 2020, Art. no. 106584.

[8] K. Shao, J. Zheng, K. Huang, H. Wang, Z. Man, and M. Fu, "Finite-time control of a linear motor positioner using adaptive recursive terminal sliding mode," *IEEE Trans. Ind. Electron.*, vol. 67, no. 8, pp. 6659–6668, Aug. 2020.

[9] Z. Sun, J. Zheng, H. Wang, and Z. Man, "Adaptive fast non-singular terminal sliding mode control for a vehicle steer-by-wire system," *IET Control Theory Appl.*, vol. 11, no. 8, pp. 1245–1254, May 2017.

[10] Z. Sun, H. Xie, J. Zheng, Z. Man, and D. He, "Path-following control of mecanum-wheels omnidirectional mobile robots using nonsingular terminal sliding mode," *Mech. Syst. Signal Process.*, vol. 147, Jan. 2021, Art. no. 107128.

[11] K. Shao, J. Zheng, H. Wang, F. Xu, X. Wang, and B. Liang, "Recursive sliding mode control with adaptive disturbance observer for a linear motor positioner," *Mech. Syst. Signal Process.*, vol. 146, Jan. 2021, Art. no. 107014.

[12] W. Ha and J. Back, "A disturbance observer-based robust tracking controller for uncertain robot manipulators," *Int. J. Control, Autom. Syst.*, vol. 16, no. 2, pp. 417–425, Apr. 2018.

[13] S.-U. Lee and P. H. Chang, "Control of a heavy-duty robotic excavator using time delay control with integral sliding surface," *Control Eng. Pract.*, vol. 10, no. 7, pp. 697–711, Jul. 2002.

[14] Y. Kali, M. Saad, K. Benjelloun, and A. Fatemi, "Discrete-time second order sliding mode with time delay control for uncertain robot manipulators," *Robot. Auto. Syst.*, vol. 94, pp. 53–60, Aug. 2017.

[15] J. Kim, H. Joe, S.-C. Yu, J. S. Lee, and M. Kim, "Time-delay controller design for position control of autonomous underwater vehicle under disturbances," *IEEE Trans. Ind. Electron.*, vol. 63, no. 2, pp. 1052–1061, Feb. 2016.

[16] J. Baek, M. Jin, and S. Han, "A new adaptive sliding-mode control scheme for application to robot manipulators," *IEEE Trans. Ind. Electron.*, vol. 63, no. 6, pp. 3628–3637, Jun. 2016.

[17] J. Baek, S. Cho, and S. Han, "Practical time-delay control with adaptive gains for trajectory tracking of robot manipulators," *IEEE Trans. Ind. Electron.*, vol. 65, no. 7, pp. 5682–5692, Jul. 2018.

[18] J. Baek, W. Kwon, B. Kim, and S. Han, "A widely adaptive time-delayed control and its application to robot manipulators," *IEEE Trans. Ind. Electron.*, vol. 66, no. 7, pp. 5332–5342, Jul. 2019.

[19] M. Jin, J. Lee, P. Hun Chang, and C. Choi, "Practical nonsingular terminal sliding-mode control of robot manipulators for high-accuracy tracking control," *IEEE Trans. Ind. Electron.*, vol. 56, no. 9, pp. 3593–3601, Sep. 2009.

[20] Y. Feng, X. Yu, and Z. Man, "Non-singular terminal sliding mode control of rigid manipulators," *Automatica*, vol. 38, no. 12, pp. 2159–2167, Dec. 2002.

[21] S. T. Venkataraman and S. Gulati, "Control of nonlinear systems using terminal sliding modes," in *Proc. Amer. Control Conf.*, Jun. 1992, pp. 891–893.

[22] M. Jin, J. Lee, and K. K. Ahn, "Continuous nonsingular terminal sliding-mode control of shape memory alloy actuators using time delay estimation," *IEEE/ASME Trans. Mechatronics*, vol. 20, no. 2, pp. 899–909, Apr. 2015.

[23] M. Van, S. S. Ge, and H. Ren, "Finite time fault tolerant control for robot manipulators using time delay estimation and continuous nonsingular fast terminal sliding mode control," *IEEE Trans. Cybern.*, vol. 47, no. 7, pp. 1681–1693, Jul. 2017.

[24] Y. Wang, L. Gu, Y. Xu, and X. Cao, "Practical tracking control of robot manipulators with continuous fractional-order nonsingular terminal sliding mode," *IEEE Trans. Ind. Electron.*, vol. 63, no. 10, pp. 6194–6204, Oct. 2016.

[25] M. B. R. Neila and D. Tarak, "Adaptive terminal sliding mode control for rigid robotic manipulators," *Int. J. Autom. Comput.*, vol. 8, no. 2, pp. 215–220, May 2011.

[26] Y. Chi-Ching, "Synchronization of second-order chaotic systems via adaptive terminal sliding mode control with input nonlinearity," *J. Franklin Inst.*, vol. 349, no. 6, pp. 2019–2032, Aug. 2012.

[27] S. Mondal and C. Mahanta, "Adaptive second order terminal sliding mode controller for robotic manipulators," *J. Franklin Inst.*, vol. 351, no. 4, pp. 2356–2377, Apr. 2014.

[28] H. Wang, Z. Man, H. Kong, Y. Zhao, M. Yu, Z. Cao, J. Zheng, and M. T. Do, "Design and implementation of adaptive terminal sliding-mode control on a steer-by-wire equipped road vehicle," *IEEE Trans. Ind. Electron.*, vol. 63, no. 9, pp. 5774–5785, Sep. 2016.

[29] J. Lee, M. Jin, and K. K. Ahn, "Precise tracking control of shape memory alloy actuator systems using hyperbolic tangential sliding mode control with time delay estimation," *Mechatronics*, vol. 23, no. 3, pp. 310–317, Apr. 2013.

[30] P. H. Chang and J. W. Jeong, "Enhanced operational space formulation for multiple tasks by using time-delay estimation," *IEEE Trans. Robot.*, vol. 28, no. 4, pp. 773–786, Aug. 2012.

[31] B.-G. Park, T.-H. Kim, and M.-J. Tahk, "Time-delay control for integrated missile guidance and control," *Int. J. Aeronaut. Space Sci.*, vol. 12, no. 3, pp. 260–265, Sep. 2011.

[32] R. P. Kumar, C. S. Kumar, D. Sen, and A. Dasgupta, "Discrete time-delay control of an autonomous underwater vehicle: Theory and experimental results," *Ocean Eng.*, vol. 36, no. 1, pp. 74–81, Jan. 2009.

[33] S. Jung, T. C. Hsia, and R. G. Bonitz, "Force tracking impedance control of robot manipulators under unknown environment," *IEEE Trans. Control Syst. Technol.*, vol. 12, no. 3, pp. 474–483, May 2004.

[34] B. Armstrong, "Friction: Experimental determination, modeling and compensation," in *Proc. IEEE Int. Conf. Robot. Autom.*, Apr. 1988, pp. 1422–1427.

[35] P. H. Chang and S. H. Park, "On improving time-delay control under certain hard nonlinearities," *Mechatronics*, vol. 13, no. 4, pp. 393–412, May 2003.

[36] Z. Man, M. O'Day, and X. Yu, "A robust adaptive terminal sliding mode control for rigid robotic manipulators," *J. Intell. Robotic Syst.*, vol. 24, no. 1, pp. 23–41, Jan. 1999.

[37] H. Yin, S. Li, and H. Wang, "Sliding mode position/force control for motion synchronization of a flexible-joint manipulator system with time delay," in *Proc. 35th Chin. Control Conf. (CCC)*, Jul. 2016, pp. 6195–6200.

[38] K. Fu, R. Gonzalez, and G. Lee, *Robotics: Control Sensing. Vision and Intelligence*. New York, NY, USA: McGraw-Hill, 1987.

[39] M. Spong, S. Hutchinson, and M. Vidyasagar, *Robot Modeling and Control*. Hoboken, NJ, USA: Wiley, 2005.

[40] K. Youcef-Toumi and S.-T. Wu, "Input/Output linearization using time delay control," *J. Dyn. Syst., Meas., Control*, vol. 114, no. 1, pp. 10–19, Mar. 1992.

[41] T. C. S. Hsia, T. A. Lasky, and Z. Guo, "Robust independent joint controller design for industrial robot manipulators," *IEEE Trans. Ind. Electron.*, vol. 38, no. 1, pp. 21–25, Feb. 1991.

[42] J. Craig, *Introduction to Robotics: Mechanics and Control*. Upper Saddle River, NJ, USA: Prentice-Hall, 2005.

[43] T. Hsia, "Simple robust schemes for Cartesian space control of robot manipulators," *Int. J. Robot. Autom.*, vol. 9, no. 4, pp. 167–174, 1994.

JINSUK CHOI (Student Member, IEEE) received the B.S. degree in electrical engineering from Inha University (IU), Incheon, South Korea, in 2015, and the M.S. degree from the School of Electrical Engineering, IU, in 2017. He is currently pursuing the Ph.D. degree with the Department of Creative IT Engineering, POSTECH, Pohang, South Korea. His research interests include computer aided control system designs, motor control systems, time-delay control, and mobile control systems.

JAEMIN BAEK (Member, IEEE) received the B.S. degree in mechanical engineering from Korea University, Seoul, South Korea, in 2012, and the Ph.D. degree (M.S.-Ph.D. joint program) in creative IT engineering from the Pohang University of Science and Technology (POSTECH), in 2018.

From 2018 to 2020, he was with the Agency for Defense Development (ADD), Daejeon, South Korea. Since 2020, he has been with the Department of Mechanical Engineering, Gangneung-Wonju National University (GWNU), Wonju, South Korea. His main research interests include controller design for nonlinear control, adaptive/robust control, and attitude control of robots, gimbals, missiles, and satellite systems.

Dr. Baek is a member of the IEEE Industrial Electronics Society, the IEEE Control Systems Society, and the Institute of Control, Robotics and Systems.

WOONGYONG LEE received the B.S. degree in mechanical engineering from Sungkyunkwan University, Seoul, South Korea, in 2012, and the Ph.D. degree in mechanical engineering from the Robotics Laboratory, Pohang University of Science and Technology (POSTECH), Pohang, South Korea, in 2020.

He is currently a Researcher with Nueromeka, a cooperative robot company, Seoul. His research interests include the development and robust control of electric and electro-hydraulic systems, and their applications to the robotic systems.

YOUNG SAM LEE (Senior Member, IEEE) received the B.S. and M.S. degrees in electrical engineering from Inha University, Incheon, South Korea, in 1999, and the Ph.D. degree in electrical engineering from Seoul National University, South Korea, in 2003. From 2003 to 2004, he was a Senior Researcher with Samsung Electronics Company Ltd. Since 2004, he has been with the Department of Electrical Engineering, Inha University. He is the author of four books and 60 articles. His research interests include computer-aided control system designs, rapid control prototyping, control and instrumentation, robot engineering, and embedded systems.

SOOHEE HAN (Senior Member, IEEE) received the B.S. degree in electrical engineering and the M.S. and Ph.D. degrees in electrical engineering and computer science from Seoul National University (SNU), Seoul, South Korea, in 1998, 2000, and 2003, respectively. From 2003 to 2007, he was a Researcher with the Engineering Research Center for Advanced Control and Instrumentation, SNU. In 2008, he was a Senior Researcher with the Robot S/W Research Center. From 2009 to 2014, he was with the Department of Electrical Engineering, Konkuk University, Seoul. Since 2014, he has been with the Department of Creative IT Engineering, Pohang University of Science and Technology, Pohang, South Korea. His research interests include reinforcement learning, autonomous vehicles, instrumentation, and battery modeling.